Available online at www.sciencedirect.com

SCIENCE DIRECT®

Carbohydrate Polymers 61 (2005) 174–182

Carbohydrate Polymers

www.elsevier.com/locate/carbpol

Innovative plasticized starch films modified with waterborne polyurethane from renewable resources

Yongshang Lu[a], Lan Tighzert[a,*], Françoise Berzin[a], Sébastien Rondot[b]

[a]*Centre d' Etudes et de Recherche en Matériaux et Emballage, Ecole Supérieure d'Ingénieurs en Emballage et Conditionnement, Esplanade Roland Garros-Pôle Henri-Farman, BP 1029, 51686 Reims cedex 2, France*

[b]*Unité de Thermique et Analyse Physique/Laboratoire des Solides Surfaces et Interfaces (UTAP/LASSI) EA3802, Université de Reims Champagne-Ardenne, 51687 Reims cedex 2, France*

Received 11 January 2005; revised 21 March 2005; accepted 22 April 2005
Available online 13 June 2005

Abstract

To develop biodegradable materials with high performance, we prepared a novel waterborne polyurethane (PU) from rapeseed oil based polyol, and then used it to modify the glycerol plasticized starch (PS) to overcome the intrinsic drawbacks of the starch materials, such as poor mechanical properties and water sensitivity. The blend films were successfully prepared by casting the aqueous dispersions of gelatinized starch and PU. The effect of PU content on the morphology, miscibility and physical properties of the resulting materials was detailed investigated by scanning electron microscopy, differential scanning calorimetry, dynamic mechanical thermal analysis and measurements of mechanical properties and water sensitivity. The results show that glycerol plasticized starch can mix with rapeseed oil based waterborne polyurethane at molecular level when PU content is lower than 20 wt%, whereas the phase separation occurs when the PU content further increases in the blends. The occurrence of hydrogen bonding interaction between starch and PU plays a key role in improvement of the material performance. Compared with the pure PS films, the PS/PU blends exhibit higher values of the elongation at break (85–480%), the toughness (1.8–7.1 MPa) and the tensile strength (2.8–4.1 MPa). Meanwhile, incorporating PU into the plasticized starch matrix leads to an improvement of surface and bulk-hydrophobation and a better water resistance of the resulting materials.

Keywords: Starch; Polyurethane

1. Introduction

The development of plastics using renewable resources which are naturally biodegradable and the possibility of combining their biodegradability with cost reduction and market needs has been the object of intensive academic and industrial research (Carvalho, Job, Alves, Curvelo, & Gandini, 2003). However, up to now the biodegradable polymers cannot be used for wide applications because of their limitations either in prices or properties. Among many kinds of candidates including aliphatic polyesters, natural polymers and their derivatives, starch, a polysaccharide produced by many plants as a storage polymer, is one of the most promising materials for biodegradable plastics because it is a versatile biopolymer with immense potential and low price for use in the non-food industries (Choi, Kim, & Park, 1999; Mohanty, Misra, & Hinrichsen, 2000). Incorporating plastifying agents, such as water and /or poly-alcohols, starch can be made into thermoplastic called thermoplastic starch (TPS) or plasticized starch (PS) through destructurization by the use of mechanical and heat energy (Ratto, Stenhouse, Auerbach, Mitchell, & Farrell, 1999). TPS has received considerable attention during past two decades and offered an interesting alternative for synthetic polymers where long-term durability is not needed and rapid degradation is an advantage (Soest, Wit, & Vliegenthart, 1996). Compared with common thermoplastics, starch based biodegradable products, unfortunately still reveal many disadvantages which are mainly attributed to the highly hydrophilic character of starch. Consequently, several strategies have been created to cope with these problems, including the modification of the starch structure (Delville, Joly, Dole, & Bliard, 2002; Zhai, Yoshii,

---

* Corresponding author. Tel.: +33 3 26913764; fax: +33 3 26913764.
E-mail address: lan.tighzert@univ-reims.fr (L. Tighzert).

0144-8617/$ - see front matter © 2005 Elsevier Ltd. All rights reserved.
doi:10.1016/j.carbpol.2005.04.013

& Kume, 2003), blending with other biodegradable polymers (Santayanon & Wootthikanokkhan, 2003; Willett & Doane, 2002) and incorporating reinforcers such as fibers (Dufresne & Vignon, 1998; Soykeabkaew, Supaphol, & Rujiravanit, 2004), whiskers (Anglès & Dufresne, 2000; Anglès & Dufresne, 2001; Mathew & Dufresne, 2002), and clay (Park et al., 2002; Wilhelm, Sierakowski, Souza, & Wypych, 2003).

Polyurethane (PU), an unique polymeric material with a wide range of physical and chemical properties, has been extensively tailored to meet the highly diversified demands of modern technologies such as coatings, adhesives, fiber, foams, and thermoplastic elastomers (Kim, Seo, & Jeong, 2003). Driven by the continuous reduction in costs and the control of volatile organic compound emissions, the development of waterborne polyurethane or poly (urethane-urea) formulations has dramatically increased (Nobel, 1997). The resulting water-borne polyurethane materials present many of features related to conventional organic solvent-borne ones with the advantage of low viscosity at high molecular weight, non-toxicity, and good applicability (Delpecha & Coutinho, 2000). Recently, there is a growing world wide interest in the development of vegetable oils based polyurethane, because of the low price and renewability (Lu & Zhang, 2002; Lu, Zhang, & Xiao, 2004; Zlatanić, Petrović, & Dušek, 2002). However, it is a pity that the researches on waterborne polyurethane from vegetable oil have not received much attention as far as now concerned. Rapeseed oil, triglycerides of predominantly unsaturated fatty acids as depicted in Fig. 1, is of vegetable origin from the seed of the cultivars of *Brassica napus* and *Brassica campestris* and is the third largest source of vegetable oil in the world. The utilization of the rapeseed oil has recently become very widespread, including end products that range from margarine to a refined biodiesel fuel, and from environmentally friendly lubricants to meal for livestock. In this work, we intend to synthesize a novel waterborne polyurethane using rapeseed oil based polyol depicted in Fig. 1 as soft segment, and then use it to modify the plasticized starch to prepare novel biodegradable materials with high performances. The effect of content of this novel waterborne polyurethane on the morphology, structure and properties of the resulting materials was investigated in detail.

2. Experimental section

2.1. Materials

Wheat starch with 25 wt% amylose and 75 wt% amylopectin was obtained from Chamtor (France), and the residual protein content was less than 1 wt%. Epoxidized rapeseed oil (100 g, 0.252 mol of oxirane) was supplied by ARD-Banzancourt, France. The glycerol (99.5% purity), hydrochloric acid (37.3%), acetone, isophorone diisocyanate (IPDI), Dimethylol propionic acid (DMPA) and triethylamine (TEA) were purchased from Aldrich and used as received.

2.2. Synthesis of chlorinated rapeseed oil polyol

Hydrochloric acid (40 g, 0.4 mol) and acetone (150 mL) were mixed in a flask equipped with a mechanical stirrer and dropping funnel. The resulting mixture was stirred vigorously, while the epoxidized rapeseed oil (100 g, 0.252 mol of oxirane) was added dropwise. The reaction mixture was stirred for additional 2 h at 40 °C, after that 150 mL ethyl acetate and 150 mL water were added, and two layers resulted. The organic layer was washed with water until a neutral pH was obtained, and then was dried over $MgSO_4$ and filtered. Finally, the organic solvent was removed by rotavapor and a yellow viscous liquid (107.3 g) was obtained. The density of the resulting chlorinated rapeseed oil polyol was determined to be 1.021 g/cm^3 by pycnometer method. Due to the decomposition of the halogenated polyol

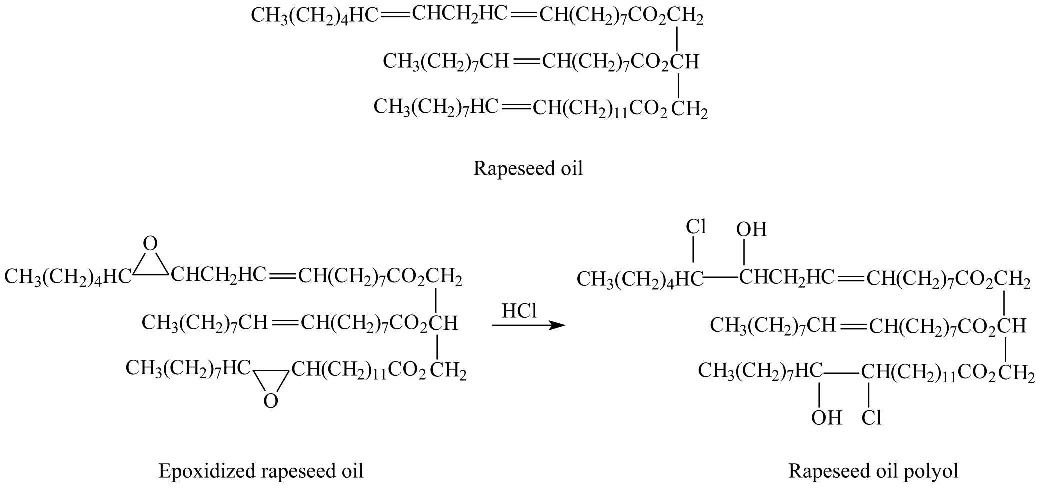

Fig. 1. Schematic representation of the ring-opening reaction of epoxidized rapeseed oil with hydrochloric acid.

during the preparation, the lower hydroxyl values maybe result (Guo, Cho, & Petrvić, 2000). Therefore, for determination of the hydroxyl values of the polyol, we use the elemental analysis instead of the titrimetric method. Elemental analysis (CHN-O-RAPID Heraeus Co., Germany) found 7.78% chlorine presents in the polyol (8.19% calculated), indicating a chlorohydrin yield of 94.5%.

2.3. Synthesis of waterborne polyurethane dispersion

Desired weight of chlorinated rapeseed oil polyol, IPDI, and DMPA were charged into a four-necked flask equipped with mechanical stirrer, nitrogen inlet, condenser and thermometer, and the reaction was carried out at 90 °C for 4 h at dry nitrogen atmosphere. After that the reaction was cooled to be about 40 °C and the acetone was added to reduce the viscosity of prepolymer while being stirred vigorously. The carboxylic groups of DMPA were neutralized by reaction with TEA at about 40 °C. Finally, under vigorous stirring the product was dispersed with distilled water to obtain 10 wt% transparent polyurethane (PU) aqueous dispersion, in which the hard segment content is 38 wt%.

2.4. Preparation of plasticized starch (PS)/PU films

Starch and glycerol were first mixed and dispersed in distilled water. The mixture contained 7 wt% wheat starch, 3 wt% glycerol and 90 wt% water. The gelatinization of starch was performed in a sealed reactor equipped with a stirrer operating at 100 °C for 20 min. The resulting starch pastes were cooled down to 70 °C in order to prevent evaporation of water. Subsequently, the polyurethane dispersion was added and stirred for 20 min. After mixing, the mixture was degassed under vacuum and cast in a polystyrene mold, followed by drying in an oven at 40 °C and 50% relatively humidity. By changing the content of PU dispersion of 0, 10, 20, 30, 40, 50 and 100 wt%, a series of starch/PU blend films were prepared and coded as PS, PS-10, PS-20, PS-30, PS-40, PS-50 and PU, respectively, in which the PU content was expressed on water free plasticized starch matrix. The resulting films, with a thickness of about 0.3 mm, were kept in a conditioning cabinet of 35 and 50% relative humidity (RH) at 25 °C, respectively, to ensure the equilibration of the water content in the films.

2.5. Characterizations

FT-IR spectra of epoxidized rapeseed oil, chlorinated rapeseed oil polyol and polyurethane were performed on a Nicolet Prolégé 460 FT-IR Spectrometer (Madison, USA).

The DSC analysis of the films was determined using a differential scanning calorimeter (TA2920, USA). Each sample conditioned at 50% RH was subjected to the heating/cooling cycle between −50 and 100 °C with a scanning rate 10°C/min to obtain reproducible the glass temperature (T_g) values. For a polymer, T_g was taken at the half-variation in heat capacity occurring at the glass–rubber transition. Scanning rate in the second run was 5 °C/min.

Dynamic mechanical behavior of the resulting films, with a thickness of about 0.3 mm, were determined with a dynamic mechanical thermal analyzer (TA instrument DMA 2980-USA) at 1 Hz and a heating rate of 5 °C/min in the temperature range from −90 to 100 °C. The length and width of the specimens used were 10 and 5 mm, respectively. Before experiment, the silicone wax was coated on the specimens to avoid water evaporation during scanning.

Morphology of the fractured surface of the films was investigated by a scanning electron microscopy (JEOL JSM-6100 instrument).

The tensile tests were carried out on a universal testing machine (CMT6503, Shenzhen SANS test machine Co. Ltd, China) at a tensile speed of 10 mm/min. The dumb-bell specimens of 17 mm × 4 mm (length × width) according to the ISO 1184-1983(E) standard were cut directly from the conditioned samples. The toughness of the films, namely, the fracture energy per unit volume of the sample, was obtained from the area under the corresponding tensile stress–strain curve. An average value of at least eight replicates of each material was taken.

The contact angle measurements were performed with a Kruss G23 (Germany) apparatus. A water droplet was put on the surface of a sample and the droplet shape was recorded. A CCD video camera and imagine analysis software were used to determine the contact angle evolution.

The dried films of 20 mm × 10 mm, kept at 0% RH (P_2O_5) for one week, were weighed and then conditioned in a chamber of 98%RH ($CuSO_4 \cdot 5H_2O$ saturated solution) at 25 °C. The sample was removed at desired intervals and weighed until the equilibrium state (W_∞) was reached. The water uptake of the samples was calculated as follows:

$$\text{Water uptake}(\%) = \frac{W_t - W_0}{W_0} \times 100 \qquad (1)$$

where W_0 and W_t are the initial weight and weight at time t in 98% RH of the sample, respectively.

3. Results and discussion

3.1. Chlorinated rapeseed oil polyol and polyurethane

FT-IR spectra of the epoxydized rapeseed oil, chlorinated rapeseed oil polyol and polyurethane are presented in Fig. 2. The epoxydized rapeseed oil shows the characteristic peaks at 1743, 823 and 845 cm^{-1}, assigned to the stretching vibration of carbonyl and oxirane, respectively. Compared with the spectrum of epoxydized rapeseed oil, the bands at

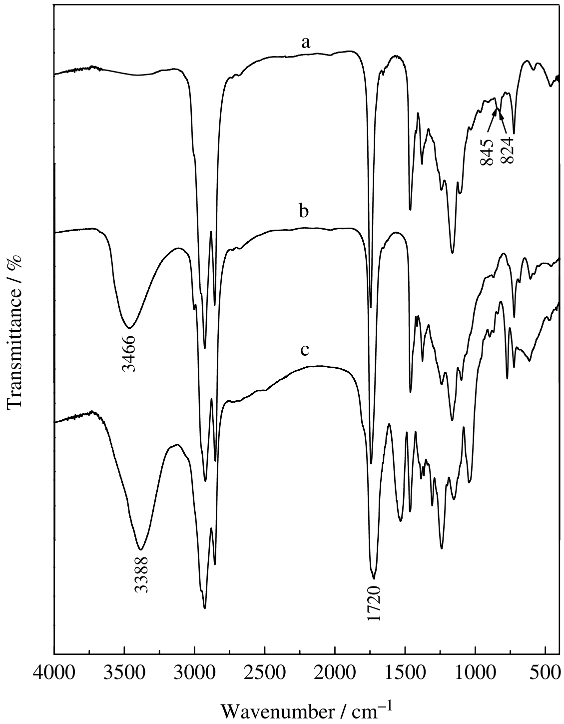

Fig. 2. FT-IR spectra of epoxidized rapeseed oil (a), chlorinated rapeseed oil polyol (b) and waterborne polyurethane (c).

823 and 845 cm^{-1} disappear while the hydroxy band at 3466 cm^{-1} occurs in spectrum of chlorinated rapeseed oil polyol. For the waterborne polyurethane prepared from the rapeseed oil based polyol, the characteristic peaks at 3384, 1720 cm^{-1}, due to stretching vibration of hydrogen-bonded -NH and hydrogen-bonded –C=O (Wang & Sung, 2002), are, respectively, observed, indicating successful preparation of water-borne polyurethane derivated from rapeseed oil based polyol.

3.2. Morphology and miscibility of the blends

The SEM images of the PS, PU and PS/PU blends are shown in Fig. 3. PS displays a one-phase morphology. The blends of PS-10 and PS-20 exhibit a relatively smooth fractured surface, indicating a high miscibility between PS and PU or good dispersion of PU phase in starch matrix. With increasing PU content, the morphology of dispersed PU phase into starch matrix is clearly observed for SP-30 and SP-50. It is indicative of phase-separated polymer blends to some extent. However, the good interfacial adhesion between PU and PS phases is also observed, which may be due to the hydrogen bonding interactions between the urethane groups of PU and the hydroxyl groups on starch.

The measurement of the glass transition temperature (T_g) of a polymer blend can provide information on the degree of polymer mixing. If the blends are immiscible, the blend will show two T_gs corresponding to the individual polymers; if there is complete miscibility between two polymer phases, only one T_g transition lying between the T_gs of the component polymers, will be observed. Broadening and shifts of the T_g transition are characteristic of partially miscible (Bikiaris, Prinos, Botev, Betchev, & Panayiotou, 2004; Biliaderis, Lazaridou, & Arvanitoyannis, 1999). The DSC curves of PS, PU and their blends in the temperature range from −30 to 100 °C are shown in Fig. 4 and the dependence of T_g on PU content is plotted in Fig. 5. PS and PU show their T_g transition at 20.4 and 44.3 °C, respectively. According to Olabisi et al. (Olabisi, Robeson, & Shaw, 1979), it is not possible to differentiate a phase-separated system from a miscible one by calorimetry if the component T_gs are less than 20 °C apart. Fortunately, substantial differences in chemical structure and relatively large difference in T_gs of about 24 °C make it possible to detect individual transitions of the component polymers by DSC. One T_g transition, lying between the T_gs of the initial polymers, is observed for PS-10 and PS-20, indicating a miscible blend of PS and PU. With a further increase in PU content, the resulting blends of PS-30 and PS-50 show two T_g transitions, corresponding respectively to the phases of PS and PU, showing that phase separation occurs in the polymer blend. It is worth noting that the T_g of each phase in the blends differs from that of the initial polymers. Further, for the blend PS-30, the T_g corresponding to PU broadens and is higher than that of pure PU. This is an indication that some specific interactions, such as hydrogen bonding between carbonyl of PU and hydroxyl of starch, are taking place, resulting in a mutual solubility of PU and PS with a concurrence of T_g difference (Parmer, Charles Dickinson, Chien, & Porter, 1989; Su, Kuo, Yei, Xu, & Chang, 2003). These interactions, however, are not strong enough to ensure the miscibility between PS and PU when PU content is more than 30 wt% in the blends. A similar observation was also reported for the styrene-*co*-maleic anhydride random copolymers (SMA)/polyacrylates blends, which is immiscible when the content of maleic anhydride groups is lower than 8 wt% (Brannock, Barlow, & Paul, 1991).

Fig. 6 shows the temperature dependence of dynamic mechanical thermal behavior for the PS/PU films. For starch film, a two-step decrease of the storage modulus and two relaxation processes of *tan*δ curve are observed at the temperatures of about −60 ($T_{\alpha 2}$) and 16 °C ($T_{\alpha 1}$), respectively. These phenomenons were also observed by other authors for starchy materials (Anglès & Dufresne, 2001; Lourdin, Bizot, & Colonna, 1997; Park et al., 2002). The starch formulation used here is a complex heterogeneous system where glycerol-rich domains are dispersed in a starch-rich continuous phase (Anglès & Dufresne, 2000; Averous & Boquillon, 2004). Each phase exhibits its own glass–rubber transition and, therefore, the relaxation processes of $T_{\alpha 1}$ and $T_{\alpha 2}$ could be, respectively, associated with glass transitions of PS (T_{g1}) and of glycerol-rich phase (T_{g2}). The rapeseed oil based PU exhibits a broad and intense *tan*δ peak of about 1.1 centered at 44.3 °C,

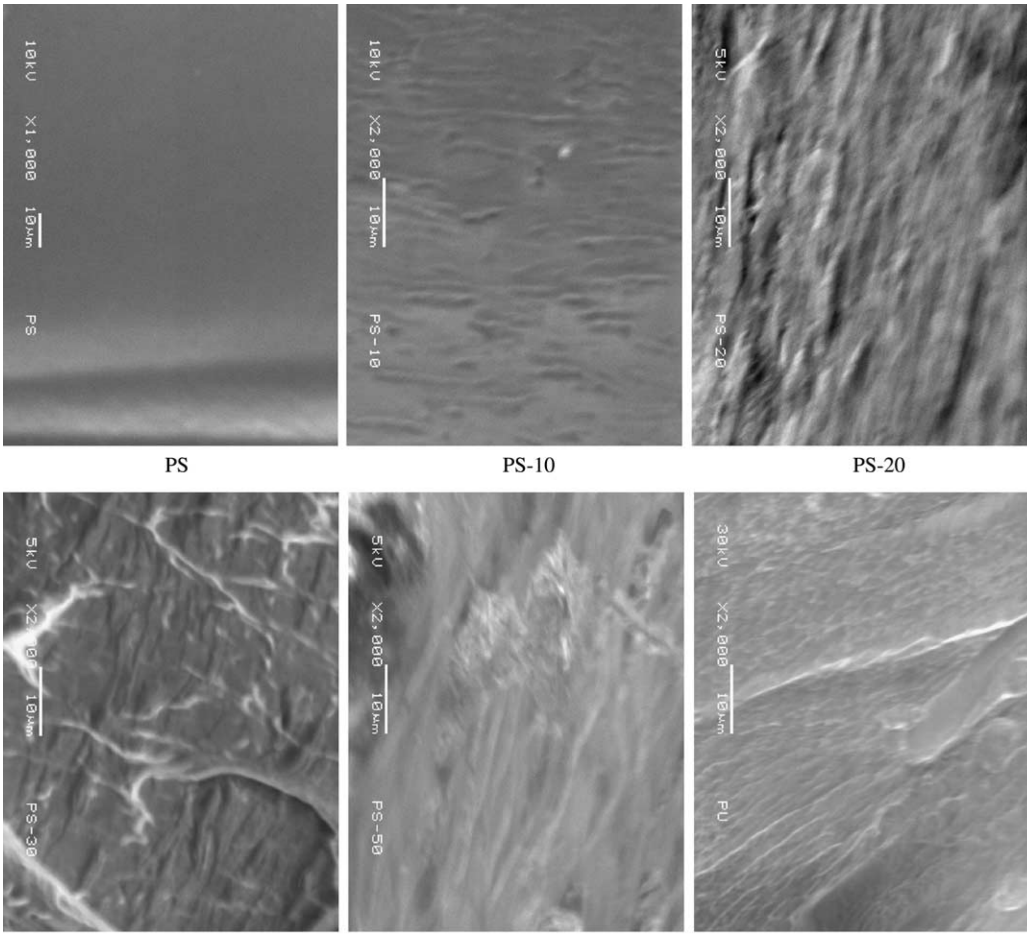

PS PS-10 PS-20

PS-30 PS-50 PU

Fig. 3. SEM image of the PS, PU and PS/PU blend films.

corresponding to its glass transition. The loss factor $\tan\delta$, a sign of the damping properties of a material, is the ratio of the mechanical dissipation energy to the storage energy. Thus a high $\tan\delta$ intensity is essential for good damping materials (Li & Larock, 2002).The rapeseed oil based PU exhibits efficient damping ability ($\tan\delta > 0.3$) over a wide temperature range from 20 to higher than 100 °C ($\Delta T >$ 80 °C), indicating that this kind of novel polyurethane has great potential for damping use. As PU is added, $\tan\delta$ curves of the resulting films display two maximum at about −75 and 25 °C, corresponding to the glass transitions of glycerol rich- and PS rich phases, respectively. The position of $T_{\alpha 2}$ relaxation is not affected by the PU content (Fig. 5) and no significant broadening of the peak is observed either, whereas the intensity of the relaxation process decreases with an increase in the PU content. Similar phenomena were also reported for the chitin whiskers reinforced natural rubber nanocomposites (Gopalan Nair & Dufresne, 2003). The intensity of the relaxation process is known to depend on both the number of mobile entities and their contribution to the compliance. On the contrary, the $T_{\alpha 1}$ relaxation process is significantly affected by incorporation of PU. The enhanced intensity and shifting to higher temperature of $T_{\alpha 1}$ relaxation peak (Fig. 5) are observed when PU content increases from 10 to 50 wt%, indicating that incorporating PU into starch does strongly influence the chain mobility of PS matrix. However, the observation of only one $T_{\alpha 1}$ relaxation is in contradiction with the visual appearance and the results of DSC of the blends. The opaque appearance of the blends with higher PU content suggests that the system is heterogeneous and two polymers may fractionate in different phases (Bikiaris et al., 2004). The observation of single $\tan\delta$ peak at about 25 °C seems surprising for the blends with higher PU content, taking into account the relatively high sensitivity of DMTA technology compared with that of DSC. However, one possible explanation is that the very slight difference in $T_{\alpha 1}$ between PS and PU phases makes it difficult to be distinguished by DMTA. The $\tan\delta$ peaks of PS and PU shift inward to each other in the blends and finally combine into an apparently single peak. So even if some interactions take place in this case, the DMTA technique could not be used safely for distinguishing the miscibility between PS and PU in this case.

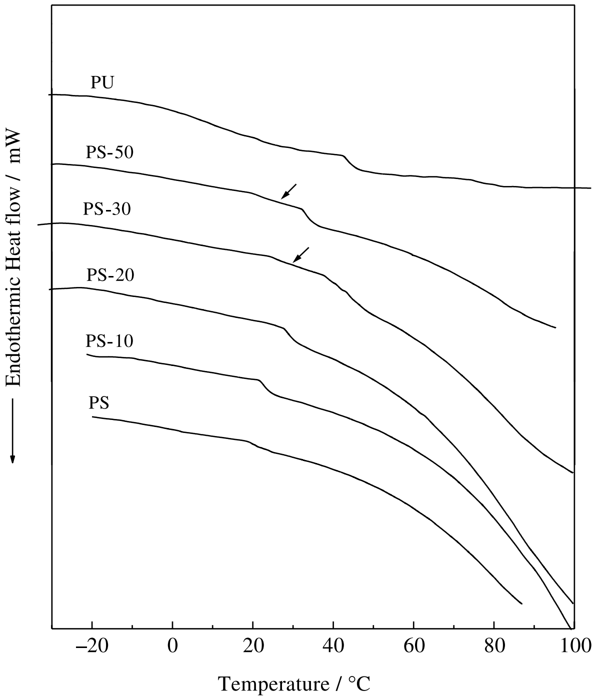

Fig. 4. DSC curves of PS, PU and PS/PU blend films.

3.3. Surface properties and water absorption

Fig. 7 shows the contact angle of the films as a function of PU content. The pure PS film exhibits a relatively low contact angle of $\theta = 37°$ at time of 0 s. The contact angle decreases rapidly, and the water droplet is totally absorbed into the starch film in less than 30 s, which confirms PS surface is hydrophilic and highly wettable. Incorporating PU into starch significantly increases the θ value from 37 to 56 °C. Furthermore, the evolution of contact angle with time is relatively slow compared with that of starch (data not shown). So the hydrophobic PU play an important role in improving surface and bulk-hydrophobation of the starch based materials, which prevents water from spreading or being absorbed (Lepifre et al., 2004).

Fig. 8 shows the water uptake of the films during conditioning in 98% RH as a function of time. The water uptake -time curves exhibit two well-separated zones. At short

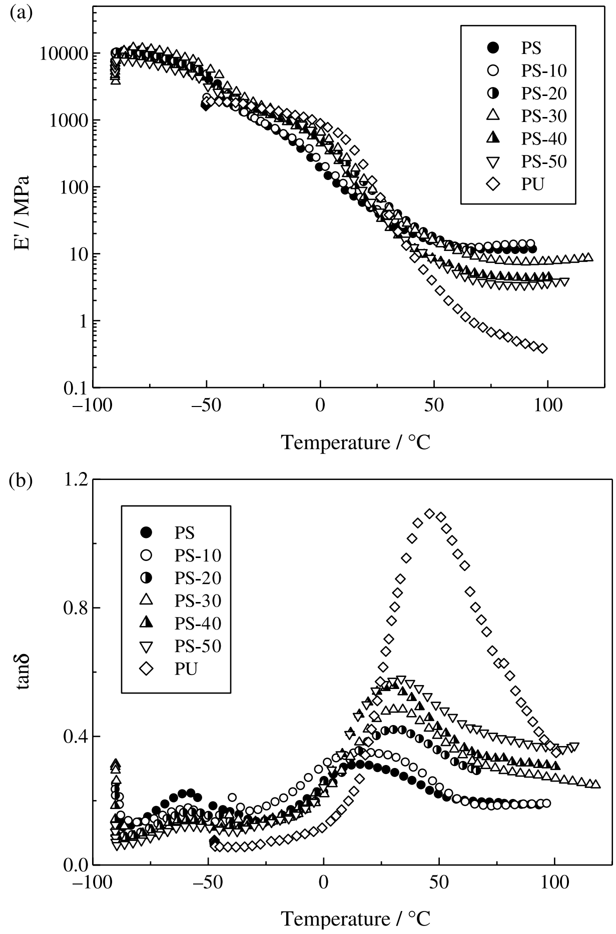

Fig. 6. Temperature dependence of storage modulus (E') and mechanical loss factor (tanδ) for PS/PU blend films.

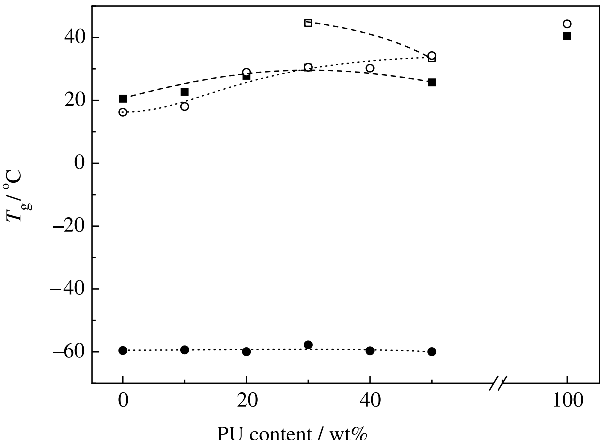

Fig. 5. The dependence of glass transition (T_g) of the PS/PU blend films measured by DSC (□, ■) and DMTA (○, ●) on the content of PU.

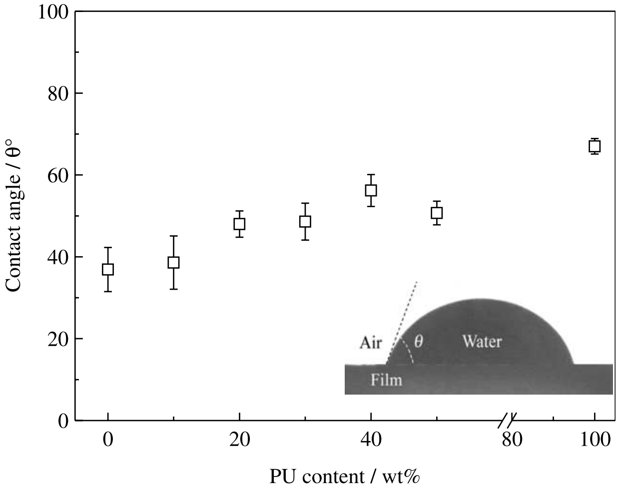

Fig. 7. Contact angle of the PS/PU blend films as a function of PU content.

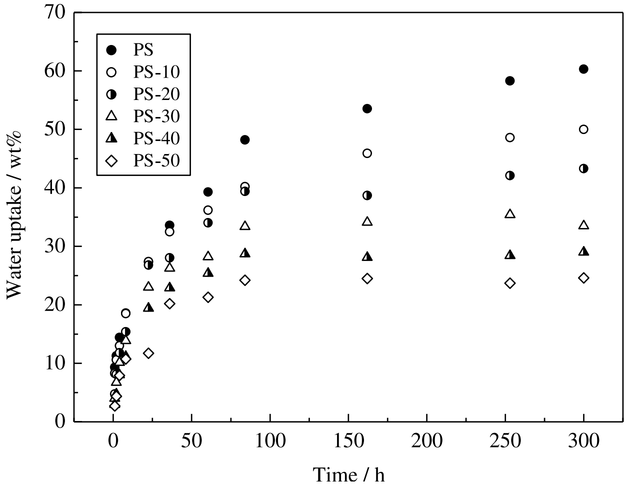

Fig. 8. Water uptake during conditioned at 98% RH versus time for PS/PU blend films.

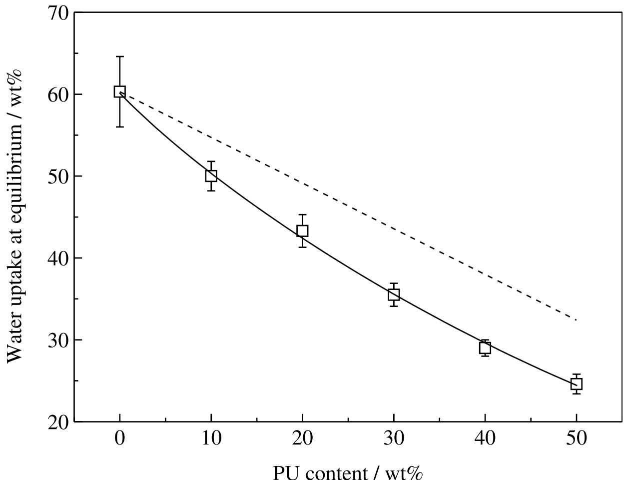

Fig. 9. Water uptake at equilibrium conditioned at 98% RH for PS/PU blend films as a function of PU content. Results are the average values of quadruplicate.

times, $t<100$ h, the kinetics of absorption is very fast, whereas at long times, $t>100$ h, the kinetics of absorption is slow and leads to a plateau, corresponding to the equilibrium of water uptake. The water uptake at equilibrium as a function of PU content for the starch-based films is plotted in Fig. 9. It is observed that the plasticized starch film absorbs about 60% water, which means about 0.6 g of water per gram of plasticized starch. The dash line is the theoretical values of equilibrium water uptake, $WU_{(\text{theorical})}$, obtained from additivity rule as the following equation:

$$WU_{(\text{theorical})} = w_{\text{PS}}WU_{\text{PS}} + w_{\text{PU}}WU_{\text{PU}}$$

Where WU and w are, respectively, the equilibrium water uptake and mass fraction in the blends. Compared with theoretical values, a lower water uptake at equilibrium is observed for the PS/PU blends, and only about 25% of water uptake for the film containing 50 wt% PU. Therefore, the swelling of the films is reduced by incorporating PU into the plasticized starch system. This phenomenon can be ascribed to the presence of strong hydrogen bonding interactions between PS matrix and PU. The hydrogen bonding interactions in the system tends to stabilize the starch matrix when it is exposed to strong moisture conditions. Meanwhile, the improvement of surface and bulk-hydrophobation of the starch-based films, resulted from addition of PU, cannot be negligible.

3.4. Mechanical properties

The data of mechanical properties for PS, PU and PS/PU blends conditioned at 35%RH and 50%RH are summarized in Table 1, and the corresponding stress–strain curves are shown in Fig. 10. The rapeseed oil based PU with the formulation in this work is an elastomeric material with a very high flexibility. Its tensile strength and elongation at break are found to be about 9.3±1.5 MPa and 520±20%, respectively. These values are very close to the results of non-biodegradable low density polyethylene with the tensile strength of 9.7–17.2 MPa and elongation at break of 500 −725% (Shah, 1984) and of PCL with tensile strength 14.2±1.4 MPa and elongation at break of about 550% (Koenig & Huang, 1995). Table 1 shows that 20–30 wt% of PU can be blended with plasticized starch before a significant decrease in tensile strength takes place. The tensile strength of the films firstly increases as the PU content increases, and reaches a maximum value (4.1 MPa at 35% RH, 3.4 MPa at 50% RH) at about 10–20 wt% of PU content. The increase in tensile strength for the PS/PU films

Table 1
The mechanical properties of PS/PU blends conditioned at 35 and 50% relative humidity, respectively

Films	35% Relative humidity			50% Relative humidity		
	Tensile strength (MPa)	Elongation at break (%)	Toughness (MPa)	Tensile strength (MPa)	Elongation at break (%)	Toughness (MPa)
PS	2.8±0.2	84.5±13	1.8±0.2	2.5±0.2	98.5±9	2.1±0.2
PS-10	3.5±0.1	124.7±10	3.5±0.3	3.4±0.3	160.4±16	4.0±0.2
PS-20	4.1±0.2	170.1±12	5.4±0.2	3.2±0.1	189.6±7	5.1±0.3
PS-30	3.3±0.2	237.5±17	6.2±0.4	2.6±0.2	263.9±20	5.5±0.2
PS-40	2.3±0.1	340.3±21	6.5±0.4	1.8±0.2	382.8±23	6.4±0.4
PS-50	1.7±0.3	478.8±15	7.1±0.4	1.5±0.3	411.9±25	5.7±0.2
PU	9.3±1.5	520.3±20	28.2±2.3	–	–	–

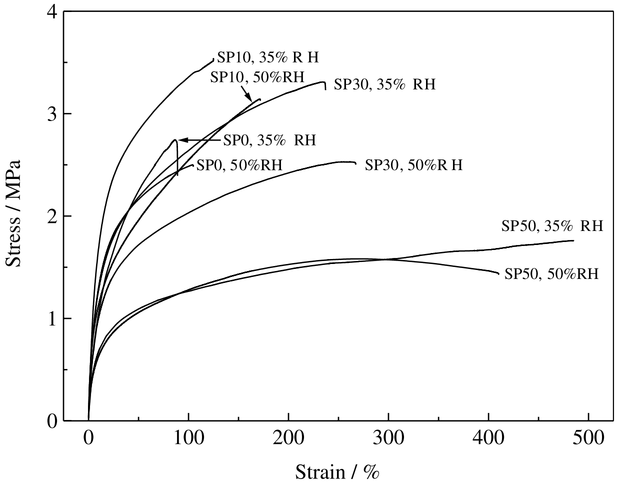

Fig. 10. The stress–strain curves of the PS/PU blend films conditioned at 35% RH and 50% RH, respectively.

indicates the occurrence of the intermolecular interaction between PU and starch. However, with increasing PU content, the tensile strength of the resulting films decreases. This can be attributed to the phase separation proved by DSC and SEM, where the domain of PU dispersed in starch rich phase grows up step by step and finally makes the PS phase non-continuous as the PU content increases from 30 to 50 wt%. In this case, the interface adhesion resulted from intermolecular interaction are not strong enough to prevent the molecular slip when the film is loaded. It is worth noting that with increasing PU content, the elongation at break of the films increases from 84 to 480% at 35% RH and from 98 to 410% at 50% RH. This is much different from the TPS/PCL and TPS/PLA blends with similar formulation at 50% RH, in which the elongation at break decreased significantly to be about 43–62% for TPS/PCL (Averous, Moro, Dole, & Fringant, 2000) and about 2–50% for TPS/PLA (Martin & Averous, 2001). Fig. 10 shows that the deformation feature of the films at room temperature under an applied load is typical of ductile plastics in terms of the stress and strain. Generally, the films exhibit two characteristic regions of deformation behavior in their tensile stress–strain curves. At low strains (<10%), the stress increases rapidly with an increase in the strain. The initial slopes were steep in the elastic region, indicating the relative high elastic moduli of the materials. At high strains (>10%), the films show a slow increase in stress with strain until failure occurs. The stress–strain curve gives not only the modulus and the strength of a material, but also its toughness. The toughness (Table 1) of the resulting starch based materials increases from 2.1 to 5.7 MPa at 50% RH and 1.8 to 7.1 MPa at 35% RH as the PU content increases from 0 to 50 wt%. Compared with that conditioned at 35%RH, the blends conditioned at 50% RH exhibit lower Young's modulus, tensile strength and higher elongation at break, due to the plasticizing effect of water molecules. Similar phenomenons were also reported for the composites of starch/poly (hydroxyester ether) (Willett & Doane, 2002) and starch/whiskers (Anglès & Dufresne, 2001).

4. Conclusions

Novel waterborne polyurethane, with good mechanical properties of both tensile strength (9.3±1.5 MPa) and elongation at break (520±20%), was successfully prepared by using rapeseed oil based polyol. By blending the PU with glycerol plasticized starch, we prepared a series of new biodegradable films based on starch with improved physical properties. When PU content is lower than 20 wt%, plasticized starch can be miscible with PU; otherwise the phase separation occurs between starch and PU. The PU significantly changes the properties of the resulting blend films. Compared with PS film, the blends show an increase in tensile strength from 2.8 to 4.1 MPa and elongation at break from 84.5 to 480% by changing the PU content, meanwhile the toughness of the materials also increases from 1.8 to 7.1 MPa at 35% RH. Further, incorporating PU into the starch matrix increases the water-resistance of the blend films. The key factor determining the enhencement of the properties of the novel PS/PU blend can be attributed to intermolecular hydrogen bonding interactions between starch and polyurethane. This work provides a new way for preparation of biodegradable materials from renewable resources.

Acknowledgements

This work is supported by Conseil Régional de Champagne-Ardenne, Conseil Général de la Marne, and la Ville de Reims through a research program devoted to the development of new biodegradable packaging materials based on starch.

References

Anglès, M. N., & Dufresne, A. (2000). Plasticized starch/tunicin whiskers nanocomposites. 1. Structural analysis. *Macromolecules*, *33*, 8344–8353.

Anglès, M. N., & Dufresne, A. (2001). Plasticized starch/tunicin whiskers nanocomposite materials. 2. Mechanical behavior. *Macromolecules*, *34*, 2921–2931.

Averous, L., & Boquillon, N. (2004). Biocomposites based on plasticized starch: Thermal and mechanical behaviours. *Carbohydrate Polymer*, *56*, 111–122.

Averous, L., Moro, L., Dole, P., & Fringant, C. (2000). Properties of thermoplastic blends: Starch–polycaprolactone. *Polymer*, *41*, 4157–4167.

Bikiaris, D., Prinos, J., Botev, M., Betchev, C., & Panayiotou, C. (2004). Blends of polymers with similar glass transition temperatures: A DMTA and DSC study. *Journal Applied Polymer Science*, *93*, 726–735.

Biliaderis, C. G., Lazaridou, A., & Arvanitoyannis, I. (1999). Glass transition and physical properties of polyol-plasticised pullulan-starch blends at low moisture. *Carbohydrate Polymer*, *40*, 29–47.

Brannock, G. R., Barlow, J. W., & Paul, D. R. (1991). Blends of styrene/maleic anhydride copolymers with polyacrylates. *Journal of Polymer Science Part B: Polymer Physics*, *29*, 413–429.

Carvalho, A. J. F., Job, A. E., Alves, N., Curvelo, A. A. S., & Gandini, A. (2003). Thermoplastic starch/natural rubber blends. *Carbohydrate Polymer*, *53*, 95–99.

Choi, E. J., Kim, C. H., & Park, J. K. (1999). Structure-property relationship in PCL/starch blend compatibilized with starch-g-PCL copolymer. *Journal of Polymer Science Part B: Polymer Physics*, *37*, 2430–2438.

Delpecha, M. C., & Coutinho, F. M. B. (2000). Waterborne anionic polyurethanes and poly(urethane-urea)s: Influence of the chain extender on mechanical and adhesive properties. *Polymer Testing*, *19*, 939–952.

Delville, J., Joly, C., Dole, P., & Bliard, C. (2002). Solid state photocrosslinked starch based films: A new family of homogeneous modified starches. *Carbohydrate Polymer*, *49*, 71–81.

Dufresne, A., & Vignon, M. R. (1998). Improvement of starch film performances using cellulose microfibrils. *Macromolecules*, *31*, 2693–2696.

Gopalan Nair, K., & Dufresne, A. (2003). Crab shell chitin whisker reinforced natural rubber nanocomposites. 2. Mechanical behavior. *Biomacromolecules*, *4*, 666–674.

Guo, A., Cho, Y., & Petrvić, Z. S. (2000). Structure and properties of halogenated and non halogenated soy-based polyols. *Journal Polymer Science Part A: Polymer Chemistry*, *38*, 3900–3910.

Kim, B. K., Seo, J. W., & Jeong, H. M. (2003). Morphology and properties of waterborne polyurethane/clay nanocomposites. *European Polymer Journal*, *39*, 85–91.

Koenig, M. F., & Huang, S. J. (1995). Biodegradable blends and composites of polycaprolactone and starch derivatives. *Polymer*, *36*, 1877–1882.

Li, F. K., & Larock, R. C. (2002). New soybean oil-styrene-divinylbenzene thermosetting coplymers—IV. Good damping properties. *Polymer for Advanced Technology*, *13*, 436–449.

Lepifre, S., Froment, M., Cazaux, F., Houot, S., Lourdin, D., Coqueret, X., et al. (2004). Lignin incorporation combined with electron-beam irradiation improves the surface water resistance of starch films. *Biomacromolecules*, *5*, 1678–1686.

Lourdin, D., Bizot, H., & Colonna, P. (1997). Antiplasticization in starch–glycerol films? *Journal Applied Polymer Science*, *63*, 1047–1053.

Lu, Y. S., & Zhang, L. N. (2002). Morphology and mechanical properties of semi-interpenetrating polymer networks from polyurethane and benzyl konjac glucomannan. *Polymer*, *43*, 3979–3986.

Lu, Y. S., Zhang, L. N., & Xiao, P. (2004). Structure, properties and biodegradability of water resistant regenerated cellulose films coated with polyurethane/benzyl konjac glucomannan semi-IPN coating. *Polymer Degradation Stability*, *86*, 51–57.

Martin, O., & Averous, L. (2001). Poly(Lactic acid): Plasticization and properties of biodegradable multiphase systems. *Polymer*, *42*, 6209–6219.

Mathew, A. P., & Dufresne, A. (2002). Morphological investigation of nanocomposites from sorbitol plasticized starch and tunicin whiskers. *Biomacromolecules*, *3*, 609–617.

Mohanty, A. K., Misra, M., & Hinrichsen, G. (2000). Biofibres, biodegradable polymers and biocomposites: An overview. *Macromolecular Materials and Engineering*, *276/277*, 1–26.

Nobel, K. L. (1997). Waterborne polyurethanes. *Progress in organic coating*, *32*, 131–136.

Olabisi, O., Robeson, L. M., & Shaw, M. T. (1979). *Polymer–polymer miscibility*. New York: Academic Press.

Park, H. M., Li, X., Jin, C. Z., Park, C. Y., Cho, W. J., & Ha, C. S. (2002). Preparation and properties of biodegradable thermoplastic starch/clay hybrids. *Macromolecular Materials Engineering*, *287*, 553–558.

Parmer, J. F., Charles Dickinson, L., Chien, J. C. W., & Porter, R. S. (1989). Miscibility of poly(methacrylate)/poly(vinyl chloride) blends. *Macromolecules*, *22*, 1078–1083.

Ratto, J. A., Stenhouse, P. J., Auerbach, M., Mitchell, J., & Farrell, R. (1999). Processing, performance and biodegradability of a thermoplastic aliphatic polyester/starch system. *Polymer*, *40*, 6777–6788.

Santayanon, R., & Wootthikanokkhan, J. (2003). Modification of cassava starch by using propionic anhydride and properties of the starch-blended polyester polyurethane. *Carbohydrate Polymer*, *51*, 17–24.

Shah, V. (Ed.). (1984). *Handbook of plastics testing technology* (p. 3). New York: Wiley, 3.

Soest, J. J. C. van, Wit, D. de, & Vliegenthart, J. F. C. (1996). Mechanical properties of thermoplastic waxy maize starch. *Journal Applied Polymer Science*, *61*, 1927–1937.

Soykeabkaew, N., Supaphol, P., & Rujiravanit, R. (2004). Preparation and characterization of jute- and flax-reinforced starch-based composite foams. *Carbohydrate Polymers*, *58*, 53–63.

Su, Y. C., Kuo, S. W., Yei, D. R., Xu, H., & Chang, F. C. (2003). Thermal properties and hydrogen onding in polymer blend of polybenzoxazine/poly(*N*-vinyl-2-pyrrolidone). *Polymer*, *44*, 2187–2191.

Wang, S. K., & Sung, C. S. P. (2002). Fluorescence and IR characterization of cure in polyurea, polyurethane, and polyurethane-urea. *Macromolecules*, *35*, 883–888.

Wilhelm, H. M., Sierakowski, M.-R., Souza, G. P., & Wypych, F. (2003). Starch films reinforced with mineral clay. *Carbohydrate Polymer*, *52*, 101–110.

Willett, J. L., & Doane, W. M. (2002). Effect of moisture content on tensile properties of starch/poly (hydroxyester ether) composite materials. *Polymer*, *43*(4413), 4420.

Zhai, M., Yoshii, F., & Kume, T. (2003). Radiation modification of starch-based plastic sheets. *Carbohydrate Polymer*, *52*, 311–317.

Zlatanić, A., Petrović, Z. S., & Dušek, K. (2002). Structure and properties of triolein-based polyurethane networks. *Biomacromolecules*, *3*, 1048–1056.